

Four-Coordinate Trispyrazolylboratomanganese and -iron Complexes with a Pyrazolato Co-ligand: Syntheses and Properties as Oxidation Catalysts

Thomas Tietz, Christian Limberg,* Reinhard Stöber, and Burkhard Ziemer^[a]

Dedicated to Professor Hans-Joachim Freund on the occasion of his 60th birthday

Abstract: A series of complexes of the type $[(\text{Tp}^{\text{R}1,\text{R}2})\text{M}(\text{X})]$ (Tp = trispyrazolylborato) with R^1/R^2 combinations $\text{Me}/t\text{Bu}$, Ph/Me , $i\text{Pr}/i\text{Pr}$, Me/Me and for $\text{M} = \text{Mn}$ or Fe coordinating $[\text{Pz}^{\text{Me},t\text{Bu}}]^-$ (Pz = pyrazolato) or Cl^- as co-ligand X has been synthesised. Although the chloride complexes were very unreactive and stable in air, the pyrazolato series was far more reactive in contact with oxidants like O_2 and $t\text{BuOOH}$. The $[(\text{Tp}^{\text{R}1,\text{R}2})\text{M}(\text{Pz}^{\text{Me},t\text{Bu}})]$ complexes proved to be active pre-catalysts for the oxidation of cyclohexene with $t\text{BuOOH}$, reaching turnover frequencies (TOFs) ranging between moderate and good in comparison to other manganese catalysts. Cyclohexene-3-one and cyclohexene-3-ol were always found to represent the main products,

with cyclohexene oxide occasionally formed as a side product. The ratios of the different oxidation products varied with the reaction conditions: in the case of a peroxide/alkene ratio of 4:1, considerably more ketone than alcohol was obtained and cyclohexene oxide formation was almost negligible, whereas a ratio of 1:10 led to a significant increase of the alcohol proportion and to the formation of at least small amounts of the epoxide. Pre-treatment of the dissolved $[(\text{Tp}^{\text{R}1,\text{R}2})\text{M}(\text{Pz}^{\text{Me},t\text{Bu}})]$ pre-catalysts with O_2 led to product distributions and TOFs that were very similar to those found in the absence

of O_2 , so that it may be argued that $t\text{BuOOH}$ and O_2 both lead to the same active species. The results of EPR spectroscopy and ESI-MS suggest that the initial product of the reaction of $[(\text{Tp}^{\text{Me},t\text{Bu}})\text{Mn}(\text{Pz}^{\text{Me},t\text{Bu}})]$ with O_2 contains a $\text{Mn}^{\text{III}}(\text{O})_2\text{Mn}^{\text{IV}}$ core. Prolonged exposure to O_2 leads to a different dinuclear complex containing three O-bridges and resulting in different TOFs/product distributions. Analogous findings were made for other complexes and formation of these overoxidised products may explain the deviation of the catalytic performances if the reactions are carried out in an O_2 atmosphere.

Keywords: catalysis • manganese • oxidation • peroxides • pyrazolates

Introduction

A significant amount of research has been carried out in the past that exploited the favourable properties of the versatile hydrotrispyrazolylborato ligands ($\text{Tp}^{\text{R}1,\text{R}2}$)^[1] in transition-metal chemistry. In the last decade these facially coordinating tripodal N_3 donors have also been increasingly employed for the complexation of metal oxo moieties in the area of bioinorganic chemistry:

$\text{Tp}^{\text{R}1,\text{R}2}$ ligands were, for instance, chosen to model histidine-rich coordination environments in certain oxygenating iron and copper enzymes,^[2] such as the tyrosinases, the soluble

methane monooxygenase, acetylacetonate dioxygenase, catechol dioxygenases, and α -ketoglutarate-dependent iron enzymes.^[3,4] In recent years, $\text{Tp}^{\text{R}1,\text{R}2}$ metal oxo research has also been extended to the element manganese, with a focus on dioxygen and peroxide reactivity.^[5–8]

In the work presented herein, we have systematically studied the behaviour of new, well-defined, electron-rich $\text{Tp}^{\text{R}1,\text{R}2}$ manganese and iron complexes in contact with oxidants as well as the reactivity of the oxidised complexes with respect to organic substrates.

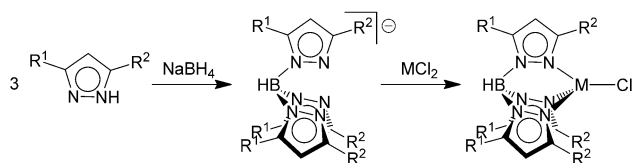
Results and Discussion

Complex synthesis and characterisation: A big advantage of the $\text{Tp}^{\text{R}1,\text{R}2}$ ligands is that the residues R^1 and R^2 can be broadly varied. In the course of our studies we found that the syntheses of the $\text{M}'\text{Tp}^{\text{R}1,\text{R}2}$ salts ($\text{M}' = \text{Na}, \text{K}$) needed as ligand precursor compounds can be significantly improved by the employment of a microwave apparatus. The reaction time can be reduced from (in some cases) three days to one hour, while yields can be increased from around 50 to around 75%. The alkali metal salts ($\text{M}'\text{Tp}^{\text{R}1,\text{R}2}$ with $\text{M}' = \text{Na},$

[a] Dipl.-Chem. T. Tietz, Prof. Dr. C. Limberg, Prof. Dr. R. Stöber, Dr. B. Ziemer
Department of Chemistry
Humboldt-Universität zu Berlin
Brook-Taylor-Strasse 2, 12489 Berlin (Germany)
Fax: (+49) 030-2093-6966
E-mail: Christian.limberg@chemie.hu-berlin.de

Supporting information for this article is available on the WWW under <http://dx.doi.org/10.1002/chem.201100343>.

K and R^1 = methyl, R^2 = phenyl or *tert*-butyl, respectively, or R^1 = R^2 = isopropyl) thus obtained were then reacted with anhydrous $MnCl_2$ in $MeOH/CH_2Cl_2$ or with anhydrous $FeCl_2$ in THF (Scheme 1) to yield the precursor complexes



Scheme 1. Synthesis of $[(Tp^{R^1,R^2})M^{II}(Cl)]$ complexes **1a**: R^1 = methyl, R^2 = *tert*-butyl, M = Mn; **1b**: R^1 = methyl, R^2 = phenyl, M = Mn; **1c**: R^1 = isopropyl, R^2 = isopropyl, M = Mn; **2a**: R^1 = methyl, R^2 = *tert*-butyl, M = Fe; **2b**: R^1 = methyl, R^2 = phenyl, M = Fe; **2c**: R^1 = isopropyl, R^2 = isopropyl, M = Fe.

$[(Tp^{R^1,R^2})M(Cl)]$ (M = Mn (**1a–c**), Fe (**2a–c**)), crystals of which could be obtained by recrystallisation of the products from toluene. As an example, the molecular structure of $[(Tp^{Me,tBu})Mn(Cl)]$ (**1a**) is shown in Figure 1. The metal ion

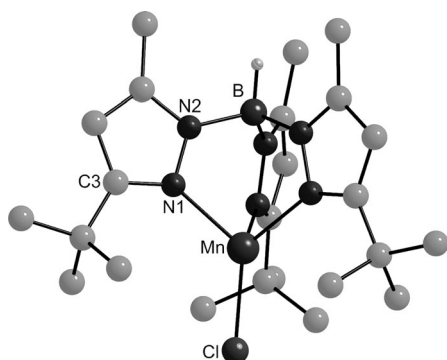


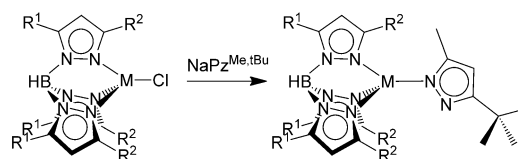
Figure 1. Molecular structure of $[(Tp^{Me,tBu})Mn(Cl)]$ (**1a**). Hydrogen atoms (except for the one belonging to the BH group) are omitted for clarity. Selected bond lengths [Å] and angles [°]: Cl–Mn 2.2863(7), Mn–N1 2.1468(10); N1–Mn–N1 91.45(4), N1–Mn–Cl 124.24(3), N2–B–N2 110.08(10).

is surrounded by the chlorido ligand and the three coordinating N atoms of the $Tp^{Me,tBu}$ ligand in a distorted tetrahedral fashion, which is reasonable for a d^5 high-spin configuration. In comparison to the ideal bond angles within a tetrahedron, the Cl–Mn–N angles are enlarged (Cl–Mn–N1: 124.24(3)°, whereas the N–Mn–N angles are reduced (N1–Mn–N1: 91.44(4)°). It is worth pointing out that the syntheses of **1a–c** in the presence of stoichiometric amounts of 3-methyl-5-*tert*-butylpyrazole ($HPz^{Me,tBu}$; Pz = pyrazolato) did not lead to the isolation of a pyrazole adduct, whereas the analogous chromium(II) compound $[(Tp^{Me,tBu})Cr(Cl)]$ coordinates $HPz^{Me,tBu}$ to give $[(Tp^{Me,tBu})Cr(Cl)(HPz^{Me,tBu})]$,^[9] presumably as this results in ligand field stabilisation in the case of the d^4 chromium atom. As this is not possible for a high-spin d^5 manganese ion and as the Lewis acidity of the manganese centres in **1a–c** apparently is not so high that the

binding of an additional ligand would be required, they prefer a tetrahedral coordination sphere.

The compounds **1b**,^[10] **1c**^[11] and **2c**^[12] had been synthesised and characterised earlier, and very recently during the preparation of this manuscript **2a** also appeared in the literature.^[13] Derivatives $[(Tp^{Me,Me})Mn(Cl)]$ and $[(Tp^{Me,Me})Fe(Cl)]$ could not be obtained, because the formation of the corresponding homoleptic complexes $[(Tp^{Me,Me})_2M]$ is favoured.

Compounds **1a–c** and **2a–c** are very unreactive. They can be crystallised in contact with air, and they are also inert towards water for longer periods of time. To increase the reactivity of the $[(Tp^{R^1,R^2})M]^+$ complex metal fragments, the chlorido ligand in **1a–c** and **2a–c** was replaced by a pyrazolato ligand $[Pz^{Me,tBu}]^-$ by reacting the compounds with the corresponding sodium salt (Scheme 2). This was supposed to



Scheme 2. Synthesis of $[(Tp^{R^1,R^2})M^{II}(Pz^{Me,tBu})]$ complexes **3a**: R^1 = methyl, R^2 = *tert*-butyl, M = Mn; **3b**: R^1 = methyl, R^2 = phenyl, M = Mn; **3c**: R^1 = isopropyl, R^2 = isopropyl, M = Mn; **4a**: R^1 = methyl, R^2 = *tert*-butyl, M = Fe; **4b**: R^1 = methyl, R^2 = phenyl, M = Fe; **4c**: R^1 = isopropyl, R^2 = isopropyl, M = Fe.

increase the electron density at the metal centre, and beyond that the more basic pyrazolato ligand (as compared to the chlorido ligand) should allow for the introduction of other (less basic) ligands in reactions with the corresponding acids.

The compounds of the type $[(Tp^{R^1,R^2})M^{II}(Pz^{Me,tBu})]$ (M = Mn (**3a–c**), Fe (**4a–c**)) obtained by this procedure were isolated and fully characterised. In the case of the complex $[(Tp^{Me,tBu})Mn(Pz^{Me,tBu})]$ (**3a**) crystals suitable for X-ray analysis were obtained, and the molecular structure of **3a** is shown in Figure 2. The manganese centre is surrounded by the four binding nitrogen atoms in a distorted tetrahedral fashion. Due to the pyrazolato ligand, the C_3 symmetry found for **1a–c** is annulled, which results in differing Mn–N bond lengths and N–Mn–N bond angles.

As the corresponding chloride precursor complexes were not available for the case of R^1 = R^2 = methyl (see above), a different synthetic strategy was developed for the preparation of $[(Tp^{Me,Me})M^{II}(Pz^{Me,tBu})]$: $MnCl_2$ or $FeCl_2$, respectively, were reacted with one equivalent of $KTp^{Me,Me}$ and one equivalent of $NaPz^{Me,tBu}$ in THF in a one-pot procedure (Scheme 3). Due to the low solubility of the undesired $[(Tp^{R^1,R^2})_2M]$ byproducts and the starting materials in THF, we were able to isolate the complexes $[(Tp^{Me,Me})Mn(Pz^{Me,tBu})]$ (**3d**) and $[(Tp^{Me,Me})Fe(Pz^{Me,tBu})]$ (**4d**) in pure form. All attempts to crystallise these compounds failed, but in the presence of excess $HPz^{Me,tBu}$ crystals of the double-pyrazole adduct of **3d** $[(Tp^{Me,Me})Mn(Pz^{Me,tBu})(HPz^{Me,tBu})_2]$ (**3d(HPz^{Me,tBu})_2**) were obtained. The result of the X-ray crys-

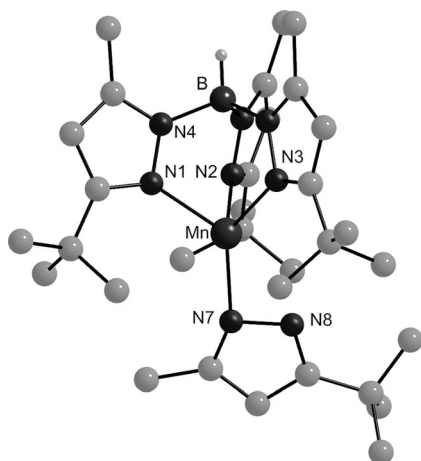
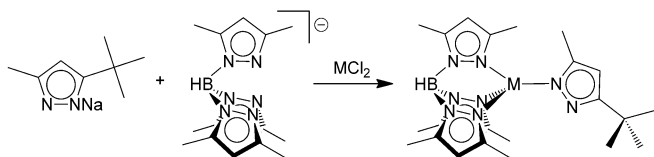


Figure 2. Molecular structure of $[(\text{Tp}^{\text{Mez,Bu}})\text{Mn}(\text{Pz}^{\text{Mez,Bu}})]$ (**3a**). Hydrogen atoms (except for the one belonging to the BH group) are omitted for clarity. Selected bond lengths [Å] and angles [°]: Mn–N1 2.1571(14), Mn–N2 2.1872(15), Mn–N3 2.1845(15), Mn–N7 2.0535(16); N1–Mn–N2 88.70(5), N1–Mn–N3 84.98(6), N2–Mn–N3 97.86(5), N1–Mn–N7 128.72(6), N2–Mn–N7 114.97(6), N3–Mn–N7 130.85(6).



Scheme 3. Synthesis of the complexes $[(\text{Tp}^{\text{Mez,Me}})\text{M}^{\text{II}}(\text{Pz}^{\text{Mez,Bu}})]$ (**3d**; M = Mn; **4d**; M = Fe).

tal structure analysis is shown in Figure 3. The manganese atom is located in a distorted octahedral coordination sphere, and its bonds to the nitrogen atoms of the coordinat-

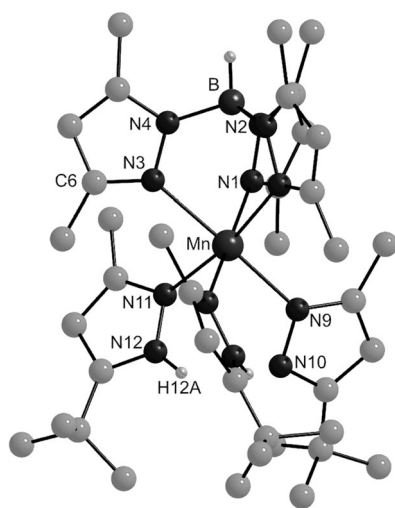


Figure 3. Molecular structure of $[(\text{Tp}^{\text{Mez,Me}})\text{Mn}(\text{Pz}^{\text{Mez,Bu}})(\text{HPz}^{\text{Mez,Bu}})_2]$ (**3d**($\text{HPz}^{\text{Mez,Bu}}_2$)). Hydrogen atoms (except for those belonging to BH and NH groups) are omitted for clarity. Selected bond lengths [Å] and angles [°]: Mn–N3 2.289(4), Mn–N9 2.197(4), Mn–N11 2.343(4); N1–Mn–N3 83.61(14), N1–Mn–N11 90.03(14), N3–Mn–N9 177.52(15), N2–B1–N4 109.2(4).

ed pyrazole ligands are significantly longer than the Mn–N bond between the manganese centre and the pyrazolato ligand.

EPR spectra of the manganese complexes **3a–d** at 77 K exhibit an intense and broad signal typical for mononuclear manganese(II) complexes (for the EPR spectrum of compound **3d**, see Figure S1 in the Supporting Information). The iron compounds **4a–d** are EPR silent at 77 K, which can be explained by a possible large zero field splitting of the high-spin d^6 centres. Crystals of **4a–d**, suitable for molecular structure analysis by means of X-ray diffraction, could not be obtained. However, a Mössbauer spectrum recorded for **4a** at room temperature showed a doublet in line with the expectations (see Figure S2 in the Supporting Information). The value for the isomeric shift of 0.823 mm s^{-1} is typical for a four-coordinate high-spin Fe^{II} centre and resembles the shift values characterising the signals of comparable complexes (see Table 1), which, however, due to distortions

Table 1. Comparison of the Mössbauer parameters of **4a** with those of similar compounds.

Compound	δ	ΔQ	Ref.
4a	0.823	0.870	
$[(\text{Ph})_2\text{B}(\text{Pz}^{\text{H,Ph}})_2\text{Fe}^{\text{II}}(\text{Cl})(\text{thf})]$	0.98	3.69	[15]
$[(\text{tha})_2\text{Fe}^{\text{II}}(\text{Cl})_2]^{\text{[a]}}$	1.09	3.28	[16]
$[(\text{thu})_2\text{Fe}^{\text{II}}(\text{Cl})_2]^{\text{[b]}}$	1.10	3.41	[16]
$(\text{NMe}_4)_2[\text{FeCl}_4]$	0.72	0.71	[14]

[a] tha = thioacetamide. [b] thu = thiocarbamide.

of the tetrahedral symmetry, often show much larger quadrupole splittings. The small quadrupole splitting found for **4a**, which is more comparable to that of the halide complex $(\text{NMe}_4)_2[\text{FeCl}_4]$,^[14] therefore indicates a quite symmetric ligand sphere, similar to that of the manganese analogues displayed in Figure 2.

Reactivity studies: As anticipated (see above), the complexes of the type $[(\text{Tp}^{\text{R1,R2}})\text{M}(\text{Pz}^{\text{Mez,Bu}})]$ (**3a–4d**) were found to be much more reactive towards oxidants than the corresponding chloride complexes **1a–2c**. However, the products obtained in reactions of **3a–4d** with O_2 in situ were not found to be powerful oxidants: only very reactive organic substrates such as tetramethylethene were oxygenated to give the corresponding epoxides. Hence, the iron and manganese complexes **3a–4d** were tested with respect to their potential to catalyse the oxidation of hydrocarbons with *t*BuOOH. Cyclohexene was chosen as the substrate as it is often used representatively for activity tests.^[17–24] Two possible pathways are known for the reaction of complex metal(II) fragments with *t*BuOOH,^[21,25] which differ from each other in the way the O–O bond of the alkyl hydroperoxide is cleaved. *Homolytic* bond cleavage results in a metal(III) hydroxido complex and an alkoxy radical that is able to abstract a hydrogen atom from the substrate, thus triggering the radical chain reaction described by Equations (1)–(10).^[26,27] These usually lead to α -hydroxyalkenes,

α,β -unsaturated carbonyl compounds and minor amounts of epoxide (often epoxides are missing completely in the product palettes).

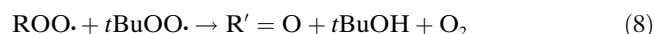
Radical chain initiation



Radical chain



Radical chain termination



Heterolytic bond cleavage results in a metal(IV) oxido complex^[21,27,28] that oxidises the organic substrate, typically leading to high yields in epoxide and hardly any α -oxidised alkenes (though Nam and co-workers proved the existence of a third principal pathway:^[25] a porphinatoiron(IV) oxido complex was shown to abstract an H atom from a second equivalent of alkyl peroxide, thereby initiating a radical chain reaction).

The catalytic oxidations with compounds **3a–4d** were carried out under two basically different sets of reaction conditions:

- 1) The concentration of oxidant used was higher than the concentration of the substrate ($[\text{tBuOOH}]/[\text{cyclohexene}] = 4:1$), and the concentration of the pre-catalyst employed was comparatively high (0.325 mol% relating to $t\text{BuOOH}$, 1.300 mol% relating to cyclohexene).
- 2) The concentration of oxidant used was lower than the concentration of the substrate ($[\text{tBuOOH}]/[\text{cyclohexene}] = 1:10$), and the concentration of the pre-catalyst employed was comparatively low (0.160 mol% relating to $t\text{BuOOH}$, 0.016 mol% relating to cyclohexene).

Irrespective of the reaction conditions, the iron and manganese complexes generated by oxidation of **3a–4d** presented herein apparently mediate the radical chain reaction

pathway, as epoxides could hardly be detected among the products.

When the reactions were carried out under the set of reaction conditions (1), almost no epoxide but only the products originating from an α oxidation of cyclohexene were obtained (Table 2 showing turnover numbers (TONs), and Figure 4 and Figure 5 showing turnover frequencies (TOFs)).

Table 2. Catalytic oxidation of cyclohexene with $t\text{BuOOH}$.^[a]

Pre-catalyst	Temperature/ solvent	Overall TON	CyEp TON	CyOH TON	CyO TON
3a	40°C/MeCN	16.9	0	2.2	14.7
3a	−40°C/MeCN	1.2	0	0.9	0.3
3a	20°C/CH ₂ Cl ₂	22.5	0	3.5	19.0
3a	−40°C/CH ₂ Cl ₂	2.7	0	1.5	1.2
3b	40°C/MeCN	24.8	0	0.8	24.0
3c	40°C/MeCN	23.9	0	2.4	21.5
3d	40°C/MeCN	13.3	0	0.8	12.5
4a	40°C/MeCN	4.6	0	1.6	3.1
4a	−40°C/MeCN	6.4	0	1.0	5.4
4a	20°C/CH ₂ Cl ₂	5.4	0	2.7	2.7
4a	−40°C/CH ₂ Cl ₂	7.8	0	2.3	5.6
4b	40°C/MeCN	5.0	0	0.5	4.6
4c	40°C/MeCN	7.2	0.2	1.2	5.8
4d	40°C/MeCN	26.9	0	3.8	23.1

[a] Catalyst concentration: 1.3 mol% with respect to alkene; ratio of peroxide/alkene = 4:1; reaction time: 2 h. CyEp: cyclohexene oxide, CyOH: cyclohexene-3-ol, CyO: cyclohexene-3-one.

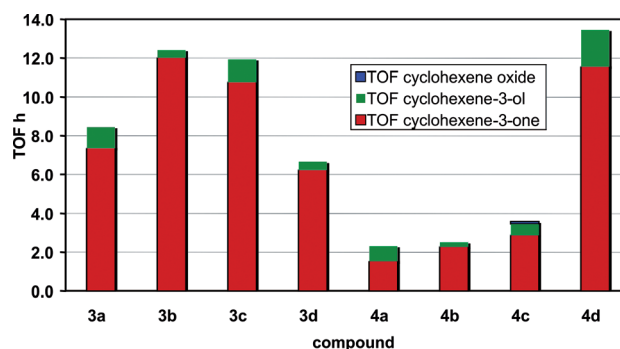


Figure 4. Turnover frequencies (TOFs) reached in the catalytic oxidation of cyclohexene with $t\text{BuOOH}$; ratio of peroxide/alkene = 4:1; catalyst concentration: 1.3 mol% with respect to cyclohexene; reaction time: 2 h; temperature: 40°C; solvent: MeCN.

The data suggest that there is no significant influence of the substituents at the $\text{Tp}^{\text{R1,R2}}$ ligands on the product distributions and only a small influence on the overall TONs of the oxidised products (only in the iron series one complex (**4d**) sticks out). Both observations can be rationalised if a radical chain reaction is responsible for the product formation. If the less polar solvent CH_2Cl_2 is employed instead of acetonitrile, TONs increase, which is plausible, too (and in accordance with literature results^[18–20,22]): Coordination of MeCN to the metal centre slows down the radical chain initiation reactions [Eqs. (1), (2)], whereas CH_2Cl_2 is a non-coordinating solvent and thus allows for free access of the oxi-

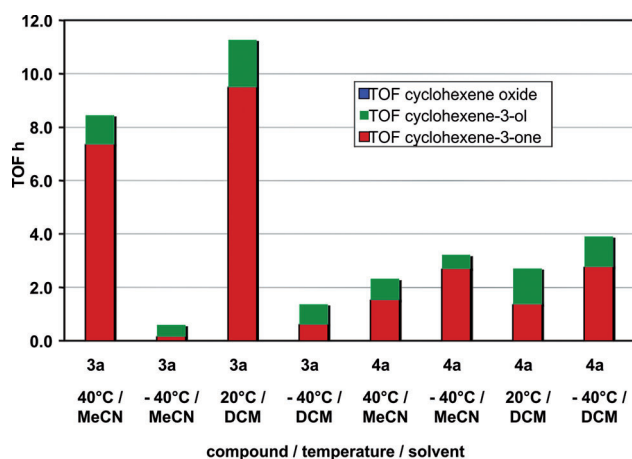


Figure 5. TOFs reached in the catalytic oxidation of cyclohexene with *t*BuOOH; ratio of peroxide/alkene=4:1; catalyst concentration: 1.3 mol% with respect to cyclohexene; reaction time: 2 h; DCM: dichloromethane.

dant to the metal centre. When *t*BuOOH is added to the prepared acetonitrile solutions containing the pre-catalysts **4a–c** at 40°C, immediate gas formation (O₂) is observed. Probably the iron catalysts formed are much more reactive than the manganese catalysts, and in combination with a high oxidant concentration Equations (3) and (4) become very dominant at 40°C, thereby resulting in the decomposition of a significant part of the oxidant, which is converted into O₂. Consistently, slowing down the reaction by cooling to –40°C prevented the formation of huge amounts of dioxygen and resulted in high TONs compared, for instance, to those observed for the corresponding manganese complex **3a**. In line with this hypothesis, reduction of the ratio of *t*BuOOH to cyclohexene led to comparatively high TONs for the same catalyst (see below).

When the reactions were carried out with the set of reaction conditions (2), again hardly any epoxide but only the products of the α oxidation of cyclohexene were obtained (Table 3 and Figure 6). However, the product distribution differed from the one observed under the reaction condi-

Table 3. Catalytic oxidation of cyclohexene with *t*BuOOH.^[a]

Pre-catalyst	Temperature/solvent	Overall TON	CyEp TON	CyOH TON	CyO TON
3a	20°C/CH ₂ Cl ₂	42.9	3.9	27.6	11.4
3a	40°C/MeCN	43.9	0	19.3	24.6
3a	40°C/MeCN/O ₂ pre-treatment	44.9	0	13.3	31.6
3a	40°C/MeCN/O ₂ as co-oxidant	53.1	3.2	49.4	0.6
4a	20°C/CH ₂ Cl ₂	88.8	4.8	38.7	45.4
4a	40°C/MeCN	106.3	3.3	35.6	67.4
4a	40°C/MeCN/O ₂ pre-treatment	114.4	4.8	47.8	61.8
4a	40°C/MeCN/O ₂ as co-oxidant	61.5	2.6	49.5	9.4

[a] Catalyst concentration: 0.16 mol% with respect to the peroxide; ratio of peroxide/alkene=1:10; reaction time: 2 h. For definitions, see Table 2.

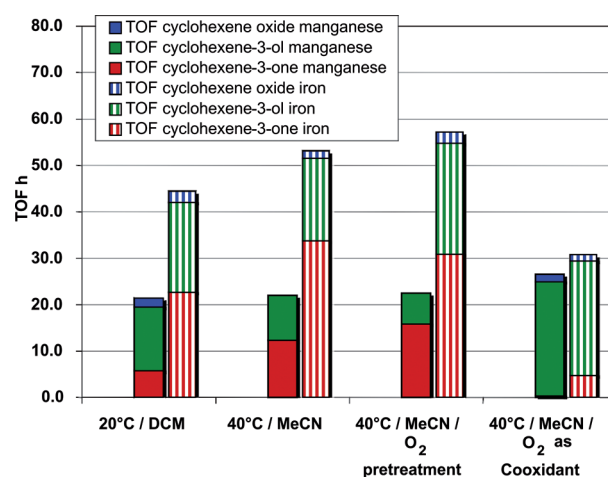


Figure 6. TOFs of the catalytic oxidation of cyclohexene with *t*BuOOH; catalysts used: **3a** (left columns), **4a** (right columns); ratio of peroxide/alkene=1:10; catalyst concentration: 0.16 mol% with respect to the peroxide; reaction time: 2 h.

tions (1): larger amounts of cyclohexene-3-ol were obtained. Apparently, at low catalyst and high substrate concentrations the reactions of the radical chain become more dominant that lead to the formation of the alcohol, and its further oxidation is suppressed.

To elucidate how far the pyrazolato co-ligands are important for the catalytic activity, complexes **1a–c** were also tested. Notably, the activity was far lower, partly only slightly above stoichiometric turnover.

The catalytically active species: Because of the high sensitivity of **3a–d** and **4a–d** towards oxidants, it is reasonable to suggest the initial formation of an oxidised complex, which then represents the active oxidation catalyst. Bubbling of O₂ through the reaction mixture prior to the addition of *t*BuOOH did not influence the yields of the oxidised products (Table 3, Figure 6), although the complexes are sensitive to O₂, so it stands to reason that identical oxidised complexes are generated by the addition of either the alkyl peroxide or O₂ (of course, in principle the O₂ product could also represent an intermediate on the way to the species formed with *t*BuOOH).

We assume that these oxidised complexes contain more than one metal centre, because Kitajima and Moro-oka showed that oxidation of the complex [(Tp^{*i*Pr,*i*Pr})Mn^{II}(μ-OH)₂Mn^{II}(Tp^{*i*Pr,*i*Pr})] (**I**) with H₂O₂ exclusively leads to the dinuclear complex [(Tp^{*i*Pr,*i*Pr})Mn^{III}(μ-O)₂Mn^{III}(Tp^{*i*Pr,*i*Pr})].^[8] A mononuclear complex with a peroxido ligand, which is coordinated side-on to the manganese centre, could only be isolated when free pyrazole (HPz^{*i*Pr,*i*Pr}) was present in solution during the oxidation reaction of **I**, so that it could saturate the coordination sphere of the manganese atom of the initial product formed.^[5] The resulting complex [(Tp^{*i*Pr,*i*Pr})Mn^{III}(HPz^{*i*Pr,*i*Pr})(O₂)] is stabilised by a hydrogen bond between the NH unit of the pyrazole ligand and the oxygen atoms of the peroxido ligand; nevertheless it decomposes rapidly at room temperature. Mononuclear iron per-

oxide complexes of the type $[\text{Fe}(\text{Tp}^{i\text{Pr},t\text{Bu}})(\text{OOH})]$ (**II**) and $[\text{Fe}(\text{Tp}^{i\text{Pr},t\text{Bu}})(\text{OO}t\text{Bu})]$ could only be obtained by employing the strongly sterically demanding $\text{Tp}^{i\text{Pr},t\text{Bu}}$ ligand at low temperatures (-80°C), as shown by the work of Moro-oka and Que and their co-workers.^[4]

The presence of larger amounts of dioxygen during the oxidation reaction seems to somewhat inhibit the formation of the ketone, whereas more cyclohexenol is formed (Table 3). One could argue that, following Equations (7) and (8), the presence of excessive dioxygen may avert the formation of the ketone, but this should generally be the case and there are differing reports in the literature.^[22,29] Hence, we assumed that an excess of dioxygen might change the catalytic centres and performed further investigations, presented below.

To obtain further information about the nature of the catalytically active species in our system, the products of the reactions of **3a–d** and **4a–d** with dioxygen were inspected more closely. In some cases over a longer period of time crystals could be grown, which, however, were very sensitive after isolation from the mother liquor so that, except for the case of **3d**, all attempts to perform an X-ray crystal structure determination failed. After oxidation of compound **3d** crystals were obtained that could be analysed, but still the solution did not reach a quality that would allow for a detailed discussion of bond lengths and angles. Nevertheless, the identity of the oxidation product **5** as a dinuclear oxygen-bridged manganese complex, as shown in Figure 7, is

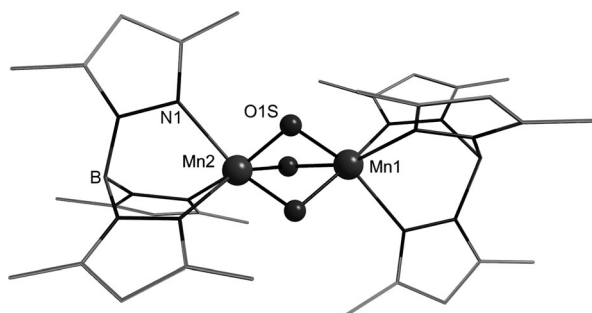


Figure 7. Heavy-atom framework of the molecular structure of **5**.

beyond doubt. To determine the nature of the bridging ligands in this oxidised complex, which does not become obvious from the X-ray data, resonance Raman spectra were recorded. Because of occurring self-heating processes or unfavourable excitation frequencies, the spectra did not reveal any reliable information. The results of investigations by infrared, mass and EPR spectroscopy suggested that the crystalline samples isolated after the oxidation of **3a–4d** with O_2 do not correspond to the catalytically active species which are formed originally from the pre-catalysts **3a–4d** under the reaction conditions used and which are responsible for the TONs in Table 2. The spectra, recorded shortly after the addition of O_2 to solutions of the pre-catalysts, differ from those of the crystalline oxidation products of **3a–4d** (Figures 8 and 9; for IR spectra, see the Supporting Information Figure S3).

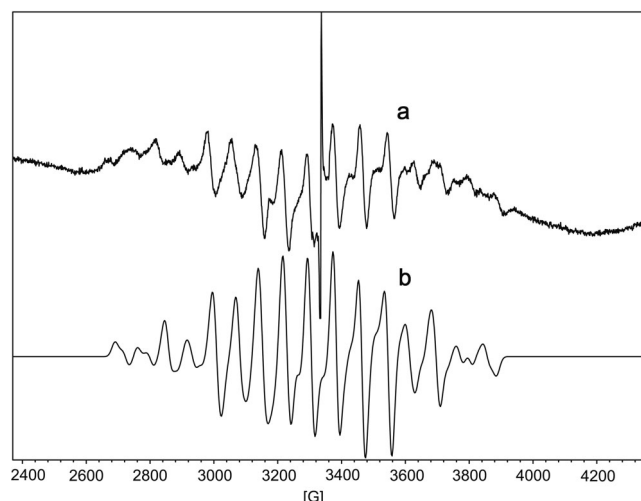


Figure 8. a) EPR spectrum of a solution of **3d** in MeCN after treatment with O_2 at 77 K and b) its simulation; $g_x = 2.0014$, $g_y = 2.0030$, $g_z = 1.9865$; $A_x[\text{Mn}^{\text{III}}] = 136.3 \times 10^{-4}$, $A_y[\text{Mn}^{\text{III}}] = 155.5 \times 10^{-4}$, $A_z[\text{Mn}^{\text{III}}] = 103.4 \times 10^{-4}$, $A_x[\text{Mn}^{\text{IV}}] = 75.3 \times 10^{-4}$, $A_y[\text{Mn}^{\text{IV}}] = 68.6 \times 10^{-4}$, $A_z[\text{Mn}^{\text{IV}}] = 77.4 \times 10^{-4} \text{ cm}^{-1}$; $S_{\text{ges}} = 1/2$.

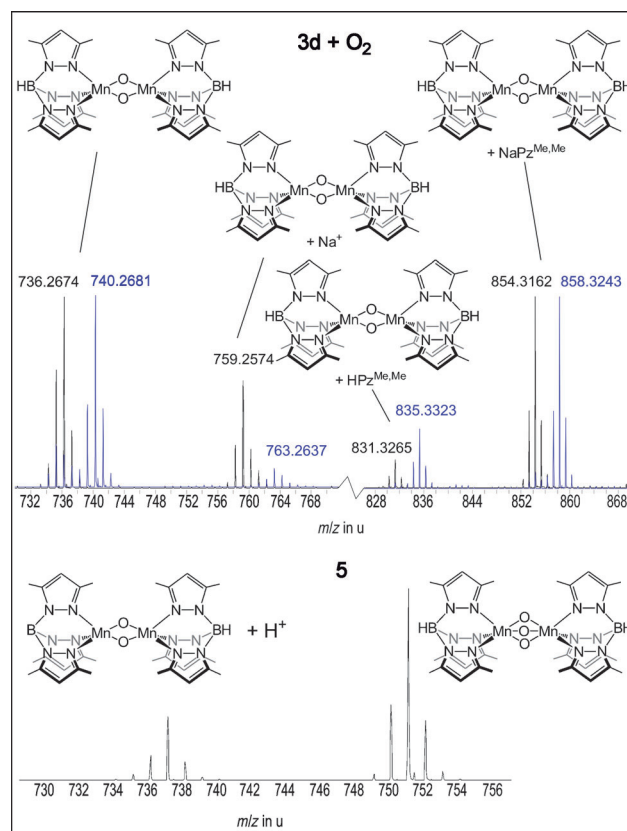


Figure 9. High-resolution mass spectra of a solution of **3d** in MeCN shortly after addition of $^{16}\text{O}_2$ (black) or $^{18}\text{O}_2$ (blue) and of a solution of **5** in MeCN.

Nevertheless, the catalytically active species generated initially appear to represent oxygen-bridged dinuclear metal complexes as well, because the EPR spectrum of a solution

of **3d** measured shortly after the addition of O₂ shows a 16 line signal, typical for dinuclear Mn^{III}–Mn^{IV} complexes^[30,31] (Figure 8). By contrast, compound **5** is EPR-silent. The high-resolution electrospray ionisation/atmospheric-pressure chemical ionisation (ESI/APCI) mass spectrum (Figure 9, top) measured shortly after the addition of O₂ to a solution of **3d** in MeCN supports the formation of a dinuclear oxido-bridged manganese(III/IV) complex, as suggested by the EPR spectra and additionally points to two bridging oxido ligands. A signal with a maximum at *m/z* 736.2674 can be assigned to the ion [(Tp^{Me,Me})Mn^{III}(O)₂Mn^{IV}(Tp^{Me,Me})]⁺; further signals can be assigned to Na⁺ and pyrazole adducts of this ion. This interpretation is corroborated by the fact that on usage of ¹⁸O₂ for the same investigation, the corresponding peaks appeared shifted by 4 mass units as expected for the incorporation of two O atoms (blue signals in Figure 9, top).^[32] The mass spectrum of **5** (Figure 9, bottom) strongly differs from the spectrum of **3d** shortly after addition of O₂. It is in agreement with the molecular structure shown in Figure 7 and suggests the constitution [(Tp^{Me,Me})Mn(O)₃Mn(Tp^{Me,Me})], as it is dominated by a peak at *m/z* 751.2692 that deviates by one mass unit from the molecular ion [(Tp^{Me,Me})Mn(O)₃Mn(Tp^{Me,Me})]⁺ and may be explained by the abstraction of H⁻ from **5** in the mass spectrometer. Besides, only one further signal can be found at *m/z* 737.2896 corresponding to [(Tp^{Me,Me})Mn^{III}(O)₂Mn^{III}(Tp^{Me,Me})]⁺ + H⁺. The conclusions drawn from these measurements are summarised in Scheme 4.

To further prove the hypothesis that the isolated oxidation products of **3a–4d**—analogues of **5**—are not the active catalysts generated from the pre-catalysts **3a–4d**, the final oxidation products of **3a** (**3aOx**) and **4a** (**4aOx**) as well as **5** were also investigated as catalysts for the oxidation of cyclohexene with *t*BuOOH under the set of reaction condi-

tions (2). The distributions of the oxidation products obtained are very different from those found in the case of **3a** or **4a** (Table 4), which indicates again that **3aOx–3cOx**, **5**

Table 4. Catalytic oxidation of cyclohexene with *t*BuOOH.^[a]

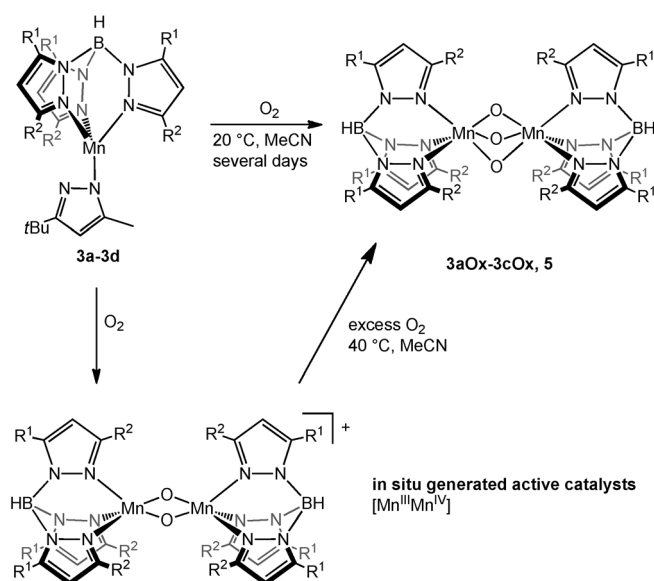
(Pre)catalyst	Temperature/solvent	Overall TON	CyEp TON	CyOH TON	CyO TON
3a	40 °C/MeCN/O ₂ as co-oxidant	53.1	3.2	49.4	0.6
3aOx	40 °C/MeCN	45.2	8.5	30.7	6.0
4a	40 °C/MeCN/O ₂ as co-oxidant	61.5	2.6	49.5	9.4
4aOx	40 °C/MeCN	89.4	13.7	58.6	17.2
5	40 °C/MeCN	168.0	12.2	77.7	78.2

[a] Catalyst concentration: 0.1–0.14 mol% with respect to the peroxide; ratio of peroxide/alkene = 1:10; reaction time: 2 h. TONs of the dinuclear complexes are calculated per metal centre for better comparison. For definitions, see Table 2

and **4aOx–4dOx** are not the active catalysts formed initially during the catalytic oxidations with *t*BuOOH, but secondary products originating from the latter after prolonged exposure to O₂. The fact that the catalytic results obtained on employment of **3aOx**, **4aOx** and **5** resemble those obtained for **3a** or **4a**, respectively, in the presence of O₂ as a co-oxidant can be explained by assuming that the formation of **3aOx–3cOx**, **5** and **4aOx–4dOx** under catalytic conditions (40 °C/O₂) is much faster than under those that had led to their isolation, so that **3aOx** and **4aOx** significantly contribute to the catalytic activity of the systems **3a/t**BuOOH/O₂ and **4a/t**BuOOH/O₂, respectively.

Conclusion

A new class of metal complexes, [(Tp^{R¹,R²})M(Pz^{Me,*t*Bu})] (M = Mn, Fe), which show a very high reactivity towards oxidants, has been synthesised and characterised. The complexes proved to be catalytically active in the oxidation of cyclohexene with *t*BuOOH to give mainly cyclohexene-3-one and cyclohexene-3-ol and minor amounts of cyclohexene oxide, respectively, and reached TOFs between average and good relative to other manganese complexes reported in the literature (Table 5). Catalysis is based on a radical-type mechanism, and hence there is only a small influence of the substituents at the Tp ligand on the TONs, which can be explained by the effect the different steric demands of the substituents have on the approach of the oxidant to the metal centre. The significant influence of the solvent can be explained along the same lines because, contrary to dichloromethane, acetonitrile can coordinate to the metal centre. Additionally, the different stabilities of the radicals formed during the reaction in the different solvents could be a reason for the different catalytic activities. The results of EPR spectroscopy as well as ESI-MS studies indicate that the active catalysts formed in situ consist of dinuclear complexes containing two bridging oxido ligands. Exposure of



Scheme 4. Proposed behaviour of the complexes **3a–d** and the catalytically active species in contact with O₂.

Table 5. Comparison of overall TOFs found for selected manganese complexes that catalyse the oxidation of cyclohexene with hydroperoxides.

Catalyst	Oxidant/conditions	Overall TOFs [h]	Ref.
3b	<i>t</i> BuOOH, MeCN, 40 °C ^[a]	12.4	
4d	<i>t</i> BuOOH, MeCN, 40 °C ^[a]	13.5	
3a	<i>t</i> BuOOH, CH ₂ Cl ₂ , 20 °C ^[a]	11.3	
3a	<i>t</i> BuOOH, CH ₂ Cl ₂ , 20 °C ^[b]	21.5	
4a	<i>t</i> BuOOH, MeCN, 40 °C ^[b]	53.2	
5	<i>t</i> BuOOH, MeCN, 40 °C ^[b]	84.5	
[(C ₈ F ₁₇)Mn{(C ₈ F ₁₇) ₃ (tacn)}]	O ₂ / <i>t</i> BuOOH, hot C ₇ F ₁₆ ^[c]	43.8	[23]
[Mn(OAc) ₃ (OPPh ₃) ₄]	<i>t</i> BuOOH, MeCN, 25 °C ^[d]	0.5	[22]
[Mn(OAc) ₃ (OPPh ₃) ₄]	O ₂ / <i>t</i> BuOOH, MeCN, 25 °C ^[e]	5.0	[22]
[Mn(OAc)(salen)]	<i>t</i> BuOOH, MeCN, 25 °C ^[d]	0.4	[22]
[Mn(OAc)(salen)]	O ₂ / <i>t</i> BuOOH, MeCN, 25 °C ^[e]	14.2	[22]
[Mn ₄ O ₄ (O ₂ PPh ₂) ₆]	<i>t</i> BuOOH, CH ₂ Cl ₂ , 25 °C ^[f]	14.0	[24]
[Mn(acac) ₂]-Al ₂ O ₃	<i>t</i> BuOOH, CH ₂ Cl ₂ , 40 °C ^[g]	0.7	[20]
[Mn(Mabenzil)]	<i>t</i> BuOOH, CH ₂ Cl ₂ , 40 °C ^[b]	51.0	[18]
[Mn(pbi)]	<i>t</i> BuOOH, cyclohexene, 60 °C ^[h]	35.0	[29]
[Mn(Cl)(tpp)]	CumylOOH, CH ₂ Cl ₂ , 20 °C ^[i]	24.0	[33]
[Mn(Cl)(tpp)]·HIm	CumylOOH, CH ₂ Cl ₂ , 20 °C ^[k]	192.0	[33]
[Mn(bpy) ₄ (OH ₂) ₂](ClO ₄) ₄	<i>t</i> BuOOH, MeCN, 0 °C ^[l]	120.3	[34]

[a] 16 μmol cat., 1.26 mmol substrate, 5 mmol *t*BuOOH, 2 h. [b] 1.6 μmol cat., 10 mmol substrate, 1 mmol *t*BuOOH, 2 h. [c] 3.5 μmol cat., 2 mL substrate, 72 μmol *t*BuOOH, excess O₂, 3 h. [d] 5 mmol cat., 1 M substrate, 20 mmol *t*BuOOH, 3 h. [e] Like [d] but additionally 1 atm O₂. [f] 0.25 mmol cat., 0.3 M substrate, 22 mmol *t*BuOOH, 1.5 h. [g] 0.74 mmol cat., 10 mmol substrate, 16 mmol *t*BuOOH, 8 h. [h] 5 μmol cat., 1 mL substrate, 2 mL *t*BuOOH, 8 h. [i] 0.1 mmol cat, stepwise per 5 mmol *t*BuOOH, reaction under air. [j] Substrate/cumylOOH/cat. = 50:5:1, 5 min. [k] Substrate/cumylOOH/cat./HIm = 50:5:1:10, 5 min. [l] 2 μmol cat., 8 mmol substrate, 16 mmol *t*BuOOH, 6 h. Tacn = triazacyclononane, acac = acetylacetonate, H₂Mabenzil = bis(2-mercaptoanil)benzil, pbi = polybenzimidazole, tpp = tetraphenylporphyrin, HIm = imidazole, bpy = 2,2'-bipyridine.

these complexes to O₂ over longer periods of time or at elevated temperatures yields dinuclear products containing three oxido bridges which, when employed as catalysts, lead to different product distributions (in favour of the alcohol).

Experimental Section

Apart from the ligand synthesis all manipulations were carried out in a glovebox, or else by means of Schlenk-type techniques involving the use of a dry argon atmosphere. ¹H and ¹³C NMR spectra were recorded on a Bruker AV 400 NMR spectrometer (¹H 400.13 MHz; ¹³C 100.63 MHz) with CDCl₃ as solvent at 20 °C. ¹H and ¹³C NMR spectra were calibrated against the residual proton and natural abundance ¹³C resonances of the deuterated solvent (CDCl₃ δ_H = 7.26, δ_C = 77.0 ppm; C₆D₆ δ_H = 7.15, δ_C = 128.0 ppm). Microanalyses were performed on a Leco CHNS-932 or HEKAtech EURO elemental analyser. ESI mass spectra were recorded on an Agilent Technologies 6210 time-of-flight LC-MS instrument. IR spectra were recorded for samples prepared as KBr pellets with a Digilab Excalibur FTS 4000 FTIR spectrometer. EPR spectra were recorded of probes within a silica glass tube on an ERS 300 X-band EPR spectrometer at 9.2 GHz. Mössbauer spectra were recorded at the Bundesanstalt für Materialforschung und -prüfung in Berlin Adlershof on a constantly accelerating Mössbauer spectrometer. The source employed was ⁵⁷Co in Pt, and the detector was a proportionality counter at 1950 V, which was calibrated with Fe₂O₃.

X-ray structure determination: The crystals were mounted on a glass fibre and then transferred into the cold nitrogen gas stream of a Stoe IPDS2T diffractometer equipped with MoK_α radiation (λ = 0.71073 Å). The structures were solved by direct methods (SIR 2004)^[35] and refined versus F2 (SHELXL-97)^[36] with anisotropic temperature factors for all non-hydrogen atoms (Table 1). All hydrogen atoms were added geometrically and refined by using a riding model. CCDC-811467 (**1a**), 811468 (**3d**) and 811469 (**3a**) contain the supplementary crystallographic data for this paper. These data can be obtained free of charge from The Cambridge Crystallographic Data Centre via www.ccdc.cam.ac.uk/data_request/cif.

Materials: Solvents were dried using a Braun Solvent Purification System. Potassium hydrotris(3,5-dimethylpyrazolyl)-borate and 3,5-diisopropylpyrazole were purchased from Aldrich; 3,5-methylphenylpyrazole,^[37] [(Tp^{Pr,IPr})Mn(Cl)]^[8] and [(Tp^{Ph,Me})Mn(Cl)]^[10] were synthesised as described earlier. The syntheses of the alkali metal hydrotrispyrazolylborate^[38] compounds of 3,5-diisopropylpyrazole, 3,5-*tert*-butylmethylpyrazole and 3,5-phenylmethylpyrazole, as well as 3,5-*tert*-butylmethylpyrazole,^[39] [(Tp^{Pr,IPr})Fe(Cl)]^[12] and [(Tp^{Me,tBu})Fe(Cl)]^[13], corresponded to published procedures.

Alkali metal hydrotrispyrazolylborate, MHB(Pz^{RLR2})₃: In a typical experiment the corresponding pyrazole (36.0 mmol, 3 equiv) was combined with the corresponding alkali metal tetrahydroborate (12.0 mmol, 1 equiv) in a Schlenk flask equipped with an excess pressure valve. The flask was then heated to 205 °C in a microwave apparatus and kept at this temperature for 60 min under vigorous stirring. After cooling the resulting light brown slurry to approximately 100 °C, toluene (ca. 30 mL) was poured into the flask. The slightly turbid solution was filtered off, and the solvent was removed at reduced pressure. Excess pyrazole was removed by means of sublimation (130 °C, 1 × 10⁻² mbar). Further sublimation of the resulting brown solid (220 °C, 8 × 10⁻³ mbar) afforded the corresponding alkali metal hydrotrispyrazolylborate in pure form (with yields ranging between 65 and 75 %) as a white solid.

Na/K[HB(Pz^{Bu,Me})₃]: ¹H NMR (400 MHz, CDCl₃): δ = 1.23 (s, 9H; *t*Bu), 2.39 (s, 3H; methyl), 5.71 ppm (s, 1H; CH); ¹³C NMR (100 MHz, CDCl₃): δ = 13.5 (CH₃^{methyl}), 30.9 (CH₃^{tBu}), 31.6 (C_q^{tBu}), 100.4 (CH^{arom.}), 143.9 (C_q^{arom.}), 160.1 ppm (C_q^{arom.}); IR (KBr): ν = 2961 (s), 2927 (s), 2904 (m), 2864 (m), 2494 (m), 1648 (m), 1539 (s), 1486 (m), 1460 (m), 1428 (m), 1361 (m), 1345 (m), 1337 (m), 1242 (m), 1183 (s), 1173 (m), 1109 (w), 1067 (s), 1023 (w), 1008 (w), 982 (w), 843 (w), 801 (m), 778 (s), 731 (w), 654 (m), 641 cm⁻¹ (m); ESI/APCI-MS (neg, THF): *m/z* (%): calcd for [Tp]⁻: 423.3443; found: 423.3374; elemental analysis calcd (%) for C₂₂H₄₀N₆BK: C 62.32, H 8.72, N 18.17; found: C 60.45, H 8.73, N 17.52.

Na/K[HB(Pz^{Pr,IPr})₃]: ¹H NMR (400 MHz, CDCl₃): δ = 1.19 (d, *J* = 6.80 Hz, 12H; CH₃^{IPr}), 2.83 (sept, *J* = 6.80 Hz, 2H; CH^{IPr}), 5.79 ppm (s, 1H; CH); ¹³C NMR (100 MHz, CDCl₃): δ = 22.6 (CH^{IPr}), 23.1 (CH₃^{IPr}), 97.8 ppm (CH^{arom.}); IR (KBr): ν = 3373 (vw), 2962 (s), 2929 (s), 2869 (m), 2464 (w), 1567 (w), 1530 (m), 1459 (m), 1424 (w), 1379 (m), 1367 (m), 1361 (m), 1302 (m), 1186 (m), 1173 (m), 1137 (w), 1105 (w), 1073 (w), 1047 (m), 1004 (m), 991 (w), 792 (s), 786 (s), 721 (w), 663 cm⁻¹ (w); ESI/APCI-MS (neg, THF): *m/z* (%): calcd for [Tp]⁻: 565.3913; found: 565.3504; elemental analysis calcd (%) for C₂₇H₄₆N₆BK: C 64.27, H 9.19, N 16.64; found: C 64.60, H 9.48, N 16.73.

Na/K[HB(Pz^{Ph,Me})₃]: ¹H NMR (400 MHz, CDCl₃): δ = 2.31 (s, 9H; methyl), 6.26 (s, 3H; CH), 7.18 (m, 1H; CH^{arom.}), 7.28 (m, 2H; CH^{arom.}), 7.54 ppm (m, 2H; CH^{arom.}); ¹³C NMR (100 MHz, CDCl₃): δ = 12.7 (CH₃^{methyl}), 102.5 (CH^{arom.}), 125.3 (CH^{Ph}), 125.5 (CH^{Ph}), 128.7 (CH^{Ph}), 131.2 (C_q^{Ph}), 143.1 (C_q^{arom.}), 149.8 ppm (C_q^{arom.}); IR (KBr): ν = 3200 (br, m), 2957 (m), 2927 (m), 2858 (m), 2449 (m), 1952 (vw), 1888 (vw), 1827 (vw), 1634 (m), 1603 (m), 1541 (m), 1508 (m), 1494 (w), 1469 (m), 1454 (m), 1429 (w), 1412 (s), 1343 (m), 1219 (m), 1177 (s), 1071 (s), 1026 (m), 961 (m), 914 (w), 841 (w), 797 (m), 763 (s), 696 (s), 661 (w), 639 cm⁻¹ (m); ESI/APCI-MS (neg, THF): *m/z* (%): calcd for [Tp]⁻: 483.2504; found: 483.2452; elemental analysis calcd (%) for C₃₀H₂₈N₆BK: C 68.96, H 5.40, N 16.08; found: C 68.82 H 5.40 N 16.07.

[(Tp^{RLR2})Mn(Cl)]: In a typical experiment a solution of the corresponding MHB(Pz^{R,R})₃ (4.2 mmol, 1 equiv) in dichloromethane was slowly added to a solution of MnCl₂ (4.2 mmol, 1 equiv) in methanol. A white

solid started to precipitate immediately, and the reaction mixture was stirred at room temperature for 48 h. Subsequently, the solvent was removed, and the resulting light brown solid was suspended in dichloromethane (15 mL) and acetonitrile (15 mL). After stirring for 30 min, the white suspension was allowed to settle for an additional 30 min before being filtered. The filtrate was concentrated to about 10 mL, which resulted in the formation of a light rose coloured precipitate. The reaction mixture was stored at -30°C for 15 h and subsequently filtered. Drying of the filter cake in a vacuum gave $[(\text{Tp}^{\text{R1,R2}})\text{Mn}(\text{Cl})]$ (with yields ranging between 50 and 70 %) as a light rose coloured solid.

$[(\text{Tp}^{\text{tBu,Me}})\text{Mn}(\text{Cl})]$ (1a): IR (KBr): $\tilde{\nu}=2935$ (s), 2930 (m), 2906 (m), 2865 (m), 2575 (m), 1537 (s), 1508 (m), 1471 (m), 1427 (m), 1382 (m), 1363 (s), 1336 (m), 1241 (m), 1180 (s), 1124 (w), 1069 (s), 1027 (m), 984 (w), 852 (w), 807 (m), 791 (s), 765 (s), 680 (w), 648 cm^{-1} (m); ESI/APCI-MS (pos, THF): m/z (%): calcd for $[\text{TpMnCl}]^{\text{H}^+}$: 514.2591; found: 514.2633; elemental analysis calcd (%) for $\text{C}_{24}\text{H}_{40}\text{N}_6\text{BMnCl}$: C 56.10, H 7.85, N 16.36, Cl 6.90; found: C 56.10, H 7.85, N 16.33, Cl 7.28.

$[(\text{Tp}^{\text{R1,R2}})\text{Fe}(\text{Cl})]$ (1b): In a typical experiment, a solution of the corresponding MHB($\text{Pz}^{\text{R,R}}$)₃ (2 mmol, 1 equiv) in THF was slowly added to a suspension of FeCl_2 (2 mmol, 1 equiv) in THF. The FeCl_2 immediately started to dissolve, and a white solid started to precipitate. The reaction mixture was stirred at room temperature for 48 h. Subsequently, the solvent was removed and the resulting light brown solid was suspended in dichloromethane (15 mL) and acetonitrile (15 mL). After stirring for 30 min the ochre suspension was allowed to settle for an additional 30 min before being filtered. The filtrate was concentrated to about 10 mL, which resulted in the formation of a light ochre coloured precipitate. The reaction mixture was stored at -30°C for 15 h and subsequently filtered. Drying of the filter cake in a vacuum gave $[(\text{Tp}^{\text{R1,R2}})\text{Fe}(\text{Cl})]$ (with yields ranging between 50 and 70 %) as a light ochre coloured solid.

$[(\text{Tp}^{\text{tBu,Me}})\text{Fe}(\text{Cl})]$ (2b): IR (KBr): $\tilde{\nu}=3274$ (m), 3061 (m), 3042 (m), 2980 (m), 2961 (m), 2927 (m), 2548 (m), 1945 (vw), 1878 (vw), 1801 (vw), 1605 (w), 1566 (m), 1543 (s), 1506 (m), 1495 (m), 1474 (s), 1450 (s), 1436 (s), 1415 (s), 1364 (m), 1341 (m), 1306 (m), 1284 (w), 1268 (w), 1192 (s), 1174 (s), 1069 (s), 1019 (m), 976 (m), 915 (m), 831 (m), 797 (m), 778 (s), 761 (s), 694 (s), 658 (m), 637 cm^{-1} (m); ESI/APCI-MS (pos, THF): m/z (%): calcd for $[\text{TpFeCl}]^{\text{H}^+}$: 575.1662; found: 575.1897; elemental analysis calcd (%) for $\text{C}_{30}\text{H}_{53}\text{N}_6\text{BFFeCl}$: C 62.70, H 4.91, N 14.62, Cl 6.17; found: C 62.95, H 5.03, N 14.27, Cl 6.54.

$[(\text{Tp}^{\text{R1,R2}})\text{Mn}(\text{Pz}^{\text{tBu,Me}})]$ (2c): In a typical experiment a solution of $\text{NaPz}^{\text{tBu,Me}}$ (192 mg, 1.2 mmol, 1 equiv) in toluene (10 mL) was added to a solution of $[(\text{Tp}^{\text{R1,R2}})\text{Mn}(\text{Cl})]$ (1.2 mmol, 1 equiv) in toluene (10 mL). The resulting slightly turbid reaction mixture was stirred at room temperature for 48 h before being filtered. The solvent of the filtrate was removed under reduced pressure and recrystallisation of the resulting light brown solid from acetonitrile at -30°C gave $[(\text{Tp}^{\text{R1,R2}})\text{Mn}(\text{Pz}^{\text{tBu,Me}})]$ (with yields ranging between 70 and 80 %) as a white solid.

$[(\text{Tp}^{\text{tBu,Me}})\text{Mn}(\text{Pz}^{\text{tBu,Me}})]$ (3a): IR (KBr): $\tilde{\nu}=2963$ (s), 2929 (s), 2907 (m), 2866 (m), 2547 (m), 1541 (m), 1465 (m), 1431 (m), 1362 (m), 1243 (m), 1185 (s), 1068 (s), 1028 (m), 1019 (m), 985 (m), 807 (m), 796 (m), 787 (m), 771 (m), 648 cm^{-1} (m); ESI-MS (pos, THF): m/z (%): calcd for $[\text{TpMn}]^{\text{H}^+}$: 478.2824; found: 478.2855; elemental analysis calcd (%) for $\text{C}_{32}\text{H}_{53}\text{N}_8\text{BMn}$: C 62.44, H 8.68, N 18.20; found: C 59.65, H 8.28, N 16.00.

$[(\text{Tp}^{\text{Ph,Me}})\text{Mn}(\text{Pz}^{\text{tBu,Me}})]$ (3b): IR (KBr): $\tilde{\nu}=3059$ (m), 2961 (m), 2926 (m), 2856 (m), 2544 (m), 1543 (s), 1505 (m), 1473 (m), 1451 (m), 1433 (m), 1415 (s), 1364 (m), 1341 (m), 1302 (w), 1259 (m), 1192 (s), 1172 (s), 1092 (m), 1067 (s), 1029 (s), 977 (m), 793 (s), 776 (s), 762 (s), 692 (s), 636 cm^{-1} (m); ESI-MS (pos, THF): m/z (%): calcd for $[\text{TpMn}]^{\text{H}^+}$: 538.1885; found: 538.1880; elemental analysis calcd (%) for $\text{C}_{38}\text{H}_{41}\text{N}_8\text{BMn}$: C 67.56, H 6.12, N 16.59; found: C 66.76, H 6.43, N 15.68.

$[(\text{Tp}^{\text{tPr,Pr}})\text{Mn}(\text{Pz}^{\text{tBu,Me}})]$ (3c): IR (KBr): $\tilde{\nu}=2960$ (s), 2927 (m), 2912 (m), 2903 (m), 2891 (m), 2866 (m), 2542 (m), 1534 (m), 1516 (w), 1473 (m), 1461 (m), 1428 (w), 1392 (m), 1381 (m), 1364 (m), 1298 (m), 1261 (w), 1170 (s), 1054 (s), 816 (m), 807 (m), 790 (s), 766 (m), 716 (w), 657 cm^{-1} (m); ESI-MS (pos, THF): m/z (%): calcd for $[\text{TpMn}]^{\text{H}^+}$: 520.3293; found: 520.3180; elemental analysis calcd (%) for $\text{C}_{35}\text{H}_{59}\text{N}_8\text{BMn}$: C 63.92, H 9.04, N 17.04; found: C 63.12, H 8.74, N 16.18.

$[(\text{Tp}^{\text{Me,Me}})\text{Mn}(\text{Pz}^{\text{tBu,Me}})]$ (3d): A solution of $\text{KHB}(\text{Pz}^{\text{Me,Me}})_3$ (500 mg, 1.49 mmol, 1 equiv) and $\text{NaPz}^{\text{tBu,Me}}$ (238 mg, 1.49 mmol, 1 equiv) in THF (10 mL) was slowly added to a stirred suspension of MnCl_2 (187 mg, 1.49 mmol, 1 equiv) in THF (5 mL). The resulting suspension was stirred at room temperature for 48 h before being filtered. The solvent of the filtrate was removed under reduced pressure and the resulting light brown solid was suspended in toluene. After stirring for 30 min, the reaction mixture was filtered. The solvent of the filtrate was removed under reduced pressure, and recrystallisation of the resulting light brown solid from acetonitrile at -30°C gave $[(\text{Tp}^{\text{Me,Me}})\text{Mn}(\text{Pz}^{\text{tBu,Me}})]$ (480 mg, 0.98 mmol, 66 %) as a white solid. IR (KBr): $\tilde{\nu}=2961$ (s), 2925 (m), 2865 (m), 2524 (m), 1541 (s), 1484 (w), 1445 (s), 1417 (s), 1380 (m), 1366 (m), 1350 (m), 1261 (m), 1203 (s), 1193 (s), 1096 (m), 1069 (s), 1038 (s), 1018 (s), 983 (w), 859(w), 840 (w), 807 s), 788 (s), 697 (m), 652 cm^{-1} (m); ESI-MS (pos, THF): m/z (%): calcd for $[\text{TpMn}]^{\text{H}^+}$: 352.1415; found: 352.1418; elemental analysis calcd (%) for $\text{C}_{23}\text{H}_{35}\text{N}_8\text{BMn}$: C 56.45, H 7.21, N 22.90; found: C 55.93, H 7.28, N 19.39.

$[(\text{Tp}^{\text{R1,R2}})\text{Fe}(\text{Pz}^{\text{tBu,Me}})]$ (4a): In a typical experiment, a solution of $\text{NaPz}^{\text{tBu,Me}}$ (192 mg, 1.2 mmol, 1 equiv) in toluene (10 mL) was added to a solution of $[(\text{Tp}^{\text{R,R}})\text{Fe}(\text{Cl})]$ (1.2 mmol, 1 equiv) in toluene (10 mL). The resulting slightly turbid reaction mixture was stirred at room temperature for 48 h before being filtered. The solvent of the filtrate was removed under reduced pressure and recrystallisation of the resulting light green solid from acetonitrile at -30°C gave $[(\text{Tp}^{\text{R1,R2}})\text{Fe}(\text{Pz}^{\text{tBu,Me}})]$ (with yield ranging between 70 and 80 %) as a white solid.

$[(\text{Tp}^{\text{tBu,Me}})\text{Fe}(\text{Pz}^{\text{tBu,Me}})]$ (4a): IR (KBr): $\tilde{\nu}=2963$ (s), 2929 (m), 2907 (m), 2864 (m), 2551 (w), 1539 (m), 1471 (m), 1465 (m), 1427 (m), 1382 (w), 1363 (m), 1346 (w), 1261 (w), 1185 (s), 1067 (s), 1028 (m), 1020 (m), 986 (w), 809(w), 786 (m), 766 (m), 648 cm^{-1} (m); ESI-MS (pos, THF): m/z (%): calcd for $[\text{TpFe}]^{\text{H}^+}$: 479.2839; found: 479.2787; elemental analysis calcd (%) for $\text{C}_{32}\text{H}_{53}\text{N}_8\text{BFFe}$: C 62.34, H 8.67, N 18.18; found: C 61.92, H 8.45, N 16.92.

$[(\text{Tp}^{\text{Ph,Me}})\text{Fe}(\text{Pz}^{\text{tBu,Me}})]$ (4b): IR (KBr): $\tilde{\nu}=3060$ (m), 2961 (m), 2925 (m), 2856 (m), 2542 (m), 1541 (s), 1505 (m), 1472 (m), 1452 (m), 1433 (m), 1416 (s), 1366 (m), 1342 (m), 1298 (w), 1260 (m), 1191 (s), 1172 (s), 1094 (m), 1067 (s), 1029 (s), 977 (m), 793 (s), 778 (s), 762 (s), 692 (s), 636 cm^{-1} (m); ESI-MS (pos, THF): m/z (%): calcd for $[\text{TpFe}]^{\text{H}^+}$: 539.1895; found: 539.2098; elemental analysis calcd (%) for $\text{C}_{38}\text{H}_{41}\text{N}_8\text{BFFe}$: C 67.47, H 6.11, N 16.57; found: C 66.55, H 6.19, N 15.87.

$[(\text{Tp}^{\text{tPr,Pr}})\text{Fe}(\text{Pz}^{\text{tBu,Me}})]$ (4c): IR (KBr): $\tilde{\nu}=2964$ (s), 2928 (m), 2869 (m), 2540 (w), 1532 (m), 1464 (m), 1419 (w), 1393 (w), 1379 (m), 1369 (m), 1300 (m), 1184 (s), 1173 (s), 1051 (s), 1026 (w), 1015 (w), 864 (w), 791 (s), 767 (w), 659 cm^{-1} (m); ESI-MS (pos, THF): m/z (%): calcd for $[\text{TpFe}]^{\text{H}^+}$: 521.3309; found: 521.2757; elemental analysis calcd (%) for $\text{C}_{35}\text{H}_{59}\text{N}_8\text{BFFe}$: C 63.83, H 9.03, N 17.02; found: C 63.27, H 8.92, N 16.35.

$[(\text{Tp}^{\text{Me,Me}})\text{Fe}(\text{Pz}^{\text{tBu,Me}})]$ (4d): A solution of $\text{KHB}(\text{Pz}^{\text{Me,Me}})_3$ (500 mg, 1.49 mmol, 1 equiv) and $\text{NaPz}^{\text{tBu,Me}}$ (238 mg, 1.49 mmol, 1 equiv) in THF (10 mL) was slowly added to a stirred suspension of FeCl_2 (189 mg, 1.49 mmol, 1 equiv) in THF (5 mL). The resulting suspension was stirred at room temperature for 48 h before being filtered. The solvent was removed under reduced pressure and the resulting light green solid was suspended in toluene. After stirring for 30 min, the reaction mixture was filtered. The solvent was removed under reduced pressure and recrystallisation of the resulting light green solid from acetonitrile at -30°C gave $[(\text{Tp}^{\text{Me,Me}})\text{Fe}(\text{Pz}^{\text{tBu,Me}})]$ (459 mg, 0.94 mmol, 63 %) as a white solid. IR (KBr): $\tilde{\nu}=3118$ (vw), 2961 (s), 2927 (m), 2887 (m), 2515 (m), 1557 (w), 1541 (s), 1521 (m), 1508 (w), 1488(w), 1447 (s), 1418 (s), 1381 (m), 1365 (m), 1350 (w), 1313 (m), 1261 (m), 1236 (w), 1203 (s), 1066 (s), 1044 (s), 1027 (s), 983 (w), 869 m), 806 (s), 778 (s), 719 (w), 695 (m), 677 m), 665 cm^{-1} (m); elemental analysis calcd (%) for $\text{C}_{23}\text{H}_{35}\text{N}_8\text{BFFe}$: C 56.35, H 7.20, N 22.86; found: C 55.59, H 7.01, N 21.92.

Catalytic oxidation of cyclohexene with *t*BuOOH and 3a–4d as pre-catalysts

Reaction conditions (I): Molecular sieves (30 mg) and successively cyclohexene (125.0 μL , 1.250 mmol), bromobenzene (62.5 μL , 0.640 mmol) and an approximately 5.5 M solution of *t*BuOOH in *n*-decane (0.91 mL, 5 mmol) were added to a solution of the pre-catalyst (16.0 μmol) in MeCN (5 mL) at 40°C . Subsequently, the solution was stirred at 40°C for

2 h before an aliquot (ca. 0.4 mL) was added to a mixture of 1–2 M HCl (2 mL) and diethyl ether (10 mL). After vigorous shaking of the mixture to transfer the metal components into the aqueous phase, an aliquot of the ethereal phase was analysed by GC-MS and GC-flame ionisation detection (FID).

Reaction conditions (2): Molecular sieves (30 mg) and successively cyclohexene (1.00 mL, 10.0 mmol), bromobenzene (20 μ L, 0.200 mmol) and an approximately 5.5 M solution of *t*BuOOH in *n*-decane (181.0 μ L, 1 mmol) were added to a solution of the pre-catalyst (1.6 μ mol) in MeCN (5 mL) at 40 °C. Subsequently, the solution was stirred at 40 °C for 2 h before an aliquot (ca. 0.4 mL) was added to a mixture of 1–2 M HCl (2 mL) and diethyl ether (10 mL). After vigorous shaking of the mixture to transfer the metal components into the aqueous phase, an aliquot of the ethereal phase was analysed by GC-MS and GC-FID.

Applied GC method: Injector: temperature at $t=0$: 50 °C; subsequently heating of the injector at 200 °C min⁻¹ until 300 °C was reached then cooling down. Column oven: temperature at $t=0$: 50 °C; subsequently holding temperature at 50 °C for 5 min; heating of the column oven at 2 °C min⁻¹ until 80 °C was reached; heating of the column oven at 100 °C min⁻¹ until 300 °C was reached; subsequently holding temperature at 300 °C for 5.80 min.

Acknowledgements

We are grateful to the Fonds der Chemischen Industrie, the BMBF and the Dr. Otto Röhm Gedächtnisstiftung for financial support as well as to Bayer Services GmbH & Co., OHG, BASF AG and Sasol GmbH for the supply of chemicals. We thank C. Knispel and P. Neubauer for crystal structure analyses and Dr. M. Menzel for Mössbauer measurements. Finally, we acknowledge helpful discussions within the Cluster of Excellence "Unifying Concepts in Catalysis" funded by the DFG.

- [1] S. Trofimenko, *Chem. Rev.* **1993**, *93*, 943; S. Trofimenko, *Scorpionates: The Coordination Chemistry of Pyrazolylborate Ligands*, Imperial College Press, London **1999**.
- [2] Y. Takano, K. Koizumi, H. Nakamura, *Inorg. Chim. Acta* **2009**, *362*, 4578; D. Diaconu, Z. Hu, S. M. Gorun, *J. Am. Chem. Soc.* **2002**, *124*, 1564; A. de la Lande, H. Gérard, V. Moliner, G. Izzet, O. Renaud, O. Parisel, *J. Biol. Inorg. Chem.* **2006**, *11*, 593; C. Diedrich, R. J. Deeth, *Inorg. Chem.* **2008**, *47*, 2494; M. Sundararajan, I. H. Hillier, N. A. Burton, *J. Phys. Chem. B* **2007**, *111*, 5511; K. Fujisawa, A. Tateda, Y. Miyashita, K.-i. Okamoto, F. Paulat, V. K. K. Praneeth, A. Merkle, N. Lehnert, *J. Am. Chem. Soc.* **2008**, *130*, 1205; C. L. Foster, X. Liu, C. A. Kilner, M. Thornton-Pett, M. A. Halcrow, *J. Chem. Soc. Dalton Trans.* **2000**, 4563; D. W. Randall, S. D. George, P. L. Holland, B. Hedman, K. O. Hodgson, W. B. Tolman, E. I. Solomon, *J. Am. Chem. Soc.* **2000**, *122*, 11632; G. Shengli, S. Liu, Y. Yuanqi, Y. Kaibe, *J. Coord. Chem.* **1998**, *46*, 145; M. A. Halcrow, L. M. L. Chia, J. E. Davies, X. Liu, L. J. Yellowlees, E. J. L. McInnes, F. E. Mabbs, *Chem. Commun.* **1998**, 2465; C. E. Ruggiero, S. M. Carrier, W. E. Antholine, J. W. Whittaker, C. J. Cramer, W. B. Tolman, *J. Am. Chem. Soc.* **1993**, *115*, 11285; M. J. Baldwin, D. E. Root, J. E. Pate, K. Fujisawa, N. Kitajima, E. I. Solomon, *J. Am. Chem. Soc.* **1992**, *114*, 10421.
- [3] L. Que, Jr., W. B. Tolman, *Angew. Chem.* **2002**, *114*, 1160; *Angew. Chem. Int. Ed.* **2002**, *41*, 1114; L. Que, Jr., W. B. Tolman, *Angew. Chem.* **2002**, *114*, 1900; *Angew. Chem. Int. Ed.* **2002**, *41*, 1821; A. Mukherjee, M. Martinho, E. L. Bominaar, E. Münck, L. Que, Jr., *Angew. Chem.* **2009**, *121*, 1812; *Angew. Chem. Int. Ed.* **2009**, *48*, 1780; T. Borowski, A. Bassan, P. E. M. Siegbahn, *Inorg. Chem.* **2004**, *43*, 3277; I. Siewert, C. Limberg, *Angew. Chem.* **2008**, *120*, 8071; *Angew. Chem. Int. Ed.* **2008**, *47*, 7953; W.-G. Han, L. Noodleman, *Inorg. Chim. Acta* **2008**, *361*, 973; T. K. Paine, H. Zheng, L. Que, *Inorg. Chem.* **2005**, *44*, 474; T. Liu, T. Lovell, W.-G. Han, L. Noodleman, *Inorg. Chem.* **2004**, *43*, 6858; M. Shoji, Y. Nishiyama, Y. Maruno, K. Koizumi, Y. Kitagawa, S. Yamanaka, T. Kawakami, M. Okumura, K. Yamaguchi, *Int. J. Quantum Chem.* **2004**, *100*, 887; A. J. Skulan, T. C. Brunold, J. Baldwin, L. Saleh, J. M. Bollinger, Jr., J. Martin, E. I. Solomon, *J. Am. Chem. Soc.* **2004**, *126*, 8842; N. Lehnert, K. Fujisawa, E. I. Solomon, *Inorg. Chem.* **2003**, *42*, 469; T. C. Brunold, N. Tamura, N. Kitajima, Y. Moro-oka, E. I. Solomon, *J. Am. Chem. Soc.* **1998**, *120*, 5674; T. Ogihara, S. Hikichi, M. Akita, Y. Moro-oka, *Inorg. Chem.* **1998**, *37*, 2614; R. C. Scarrow, M. G. Trimitsis, C. P. Buck, G. N. Grove, R. A. Cowling, M. J. Nelson, *Biochemistry* **1994**, *33*, 15023; N. Kitajima, M. Ito, H. Fukui, Y. Moro-oka, *J. Am. Chem. Soc.* **1993**, *115*, 9335; I. Siewert, C. Limberg, *Chem. Eur. J.* **2009**, *15*, 10316; M. Wagner, C. Limberg, T. Tietz, *Chem. Eur. J.* **2009**, *15*, 5567–5576.
- [4] X. Shan, J.-U. Rohde, K. D. Koehntop, Y. Zhou, M. R. Bukowski, M. Costas, K. Fujisawa, L. Que, *Inorg. Chem.* **2007**, *46*, 8410; T. Ogihara, S. Hikichi, M. Akita, T. Uchida, T. Kitagawa, Y. Moro-oka, *Inorg. Chim. Acta* **2000**, *297*, 162.
- [5] N. Kitajima, H. Komatsuzaki, S. Hikichi, M. Osawa, Y. Moro-oka, *J. Am. Chem. Soc.* **1994**, *116*, 11596.
- [6] J. E. Sheats, R. S. Czernuszewicz, G. C. Dismukes, A. L. Rheingold, V. Petrouleas, J. Stubbe, W. H. Armstrong, R. H. Beer, S. J. Lippard, *J. Am. Chem. Soc.* **1987**, *109*, 1435.
- [7] N. Kitajima, M. Osawa, M. Tanaka, Y. Moro-oka, *J. Am. Chem. Soc.* **1991**, *113*, 8952.
- [8] N. Kitajima, U. P. Singh, H. Amagai, M. Osawa, Y. Moro-oka, *J. Am. Chem. Soc.* **1991**, *113*, 7757.
- [9] K. Qin, C. D. Incarvito, A. L. Rheingold, K. H. Theopold, *Angew. Chem.* **2002**, *114*, 2439; *Angew. Chem. Int. Ed.* **2002**, *41*, 2333.
- [10] U. P. Singh, P. Tyagi, S. Upreti, *Polyhedron* **2007**, *26*, 3625.
- [11] N. Kitajima, M. Osawa, N. Tamura, Y. Moro-oka, T. Hirano, M. Hirobe, T. Nagano, *Inorg. Chem.* **1993**, *32*, 1879.
- [12] N. Kitajima, H. Fukui, Y. Moro-oka, Y. Mizutani, T. Kitagawa, *J. Am. Chem. Soc.* **1990**, *112*, 6402.
- [13] F. A. Jové, C. Pariya, M. Scoble, G. P. A. Yap, K. H. Theopold, *Chem. Eur. J.* **2011**, *17*, 1310–1318.
- [14] G. M. Bancroft, J. M. Dubery, *J. Chem. Phys.* **1969**, *50*, 2264.
- [15] M. Wagner, Dissertation thesis, Humboldt-Universität zu Berlin (Berlin), **2009**.
- [16] T. Birchall, M. F. Morris, *Can. J. Chem.* **1972**, *50*, 211.
- [17] R. van Gorkum, J. Berding, D. M. Tooke, A. L. Spek, J. Reedijk, E. Bouwman, *J. Catal.* **2007**, *252*, 110.
- [18] M. Salavati-Niasari, H. Babazadeh-Arani, *J. Mol. Catal.* **2007**, *274*, 58.
- [19] M. Salavati-Niasari, S. H. Banitaba, *J. Mol. Catal.* **2003**, *201*, 43.
- [20] M. Salavati-Niasari, F. Farzaneh, M. Ghandi, *J. Mol. Catal.* **2002**, *186*, 101.
- [21] W. Nam, S.-Y. Oh, M. H. Lim, M.-H. Choi, S.-Y. Han, G.-J. Jhon, *Chem. Commun.* **2000**, 1787.
- [22] T. Matsushita, D. T. Sawyer, A. Sobkowiak, *J. Mol. Catal.* **1999**, *137*, 127.
- [23] J.-M. Vincent, A. Rabion, V. K. Yachandra, R. H. Fish, *Angew. Chem.* **1997**, *109*, 2438.
- [24] T. G. Carrell, S. Cohen, G. C. Dismukes, *J. Mol. Catal.* **2002**, *187*, 3.
- [25] W. Nam, H. J. Han, S.-Y. Oh, Y. J. Lee, M.-H. Choi, S.-Y. Han, C. Kim, S. K. Woo, W. Shin, *J. Am. Chem. Soc.* **2000**, *122*, 8677.
- [26] P. A. MacFaul, K. U. Ingold, D. D. M. Wayner, L. Que, *J. Am. Chem. Soc.* **1997**, *119*, 10594; I. W. C. E. Arends, K. U. Ingold, D. D. M. Wayner, *J. Am. Chem. Soc.* **1995**, *117*, 4710; J. Kim, R. G. Harrison, C. Kim, L. Que, *J. Am. Chem. Soc.* **1996**, *118*, 4373.
- [27] T. L. Foster, J. P. Caradonna, *J. Am. Chem. Soc.* **2003**, *125*, 3678.
- [28] W. Nam, I. Kim, M. H. Lim, H. J. Choi, J. S. Lee, H. G. Jang, *Chem. Eur. J.* **2002**, *8*, 2067.
- [29] G. Olason, D. C. Sherrington, *React. Funct. Polym.* **1999**, *42*, 163.
- [30] K. Wiegardt, U. Bossek, B. Nuber, J. Weiss, J. Bonvoisin, M. Corbella, S. E. Vitols, J. J. Girerd, *J. Am. Chem. Soc.* **1988**, *110*, 7398.
- [31] S. Romain, C. Baffert, C. Duboc, J.-C. Leprêtre, A. Deronzier, M.-N. Collomb, *Inorg. Chem.* **2009**, *48*, 3125; R. Hage, B. Krijnen, J. B. Warnaar, F. Hartl, D. J. Stufkens, T. L. Snoeck, *Inorg. Chem.* **1995**, *34*, 4973; J. W. de Boer, P. L. Alsters, A. Meetsma, R. Hage, W. R.

- Browne, B. L. Feringa, *Dalton Trans.* **2008**, 6283; K.-O. Schäfer, R. Bittl, F. Lenzian, V. Barynin, T. Weyhermüller, K. Wieghardt, W. Lubitz, *J. Phys. Chem. B* **2003**, *107*, 1242; A. Magnuson, P. Liebisch, J. Höglblom, M. F. Anderlund, R. Lomoth, W. Meyer-Klaucke, M. Haumann, H. Dau, *J. Inorg. Biochem.* **2006**, *100*, 1234; J. W. de Boer, W. R. Browne, J. Brinksma, P. L. Alsters, R. Hage, B. L. Feringa, *Inorg. Chem.* **2007**, *46*, 6353; J. A. Lessa, A. Horn, É. S. Bull, M. R. Rocha, M. Benassi, R. R. Catharino, M. N. Eberlin, A. Casellato, C. J. Noble, G. R. Hanson, G. Schenk, G. C. Silva, O. A. C. Antunes, C. Fernandes, *Inorg. Chem.* **2009**, *48*, 4569.
- [32] A further signal at m/z 887.3598 may originate from the product of an intramolecular ligand oxidation containing two ^(Tp)B-Pz^{Me}-CH₂-O-Mn moieties and a Mn-O-Mn unit. Kitajima et al. have reported the formation of an analogous product in the reaction of [(Tp^{iPr})₂Mn(OH)₂Mn(Tp^{iPr})₂] with O₂.^[7]
- [33] D. Mansuy, P. Battioni, J.-P. Renaud, *J. Chem. Soc. Chem. Commun.* **1984**, 1255.
- [34] J. E. Sarneski, M. Didiuk, H. H. Thorp, R. H. Crabtree, G. W. Brudvig, J. W. Faller, G. K. Schulte, *Inorg. Chem.* **1991**, *30*, 2833.
- [35] SIR 2004: Program for Crystal Structure Determination, Perugia (Italy) **2005**; M. C. Burla, R. Caliandro, M. Camalli, B. Carrozzini, G. L. Casciaro, L. De Caro, C. Giacovazzo, G. Polidori, R. Spanga, *J. Appl. Crystallogr.* **2005**, *38*, 381–388.
- [36] SHELXL-97, G. M. Sheldrick, Program for Crystal Structure Refinement, University of Göttingen, Göttingen (Germany), **1997**.
- [37] D. T. Puerta, S. M. Cohen, *Inorg. Chim. Acta* **2002**, *337*, 459.
- [38] S. Trofimenko, *J. Am. Chem. Soc.* **1967**, *89*, 3165.
- [39] F. W. Swamer, C. R. Hauser, *J. Am. Chem. Soc.* **1950**, *72*, 1352; R. H. Wiley, P. E. Hexner, *Org. Synth.* **1951**, *31*, 43.

Received: January 31, 2011
Published online: July 8, 2011